INFLUENCE OF THE SPACING BETWEEN NSM-CFRP LAMINATES ON THE FLEXURAL STRENGTHENING EFFICACY OF RC SLABS

Everaldo BONALDO [1] Joaquim A. O. BARROS [1] Paulo B. LOURENÇO [1]

[1] Department of Civil Engineering, University of Minho, Portugal

Keywords: reinforced concrete slabs, flexural strengthening, near surface mounted, CFRP laminate, cover delamination, laminate spacing, strengthening efficacy.

1 INTRODUCTION

Experimental and numerical research have demonstrated that the near surface mounted (NSM) strengthening technique, based on installing CFRP laminates into thin slits opened of the concrete cover of the RC elements to strengthen, provides higher strengthening effectiveness than the externally bonded CFRP strengthening technique (EBR). However, experimental programs dealing with the use of NSM for the increase of the flexural 1] and shear [2] resistance of RC elements have shown that, increasing the CFRP strengthening ratio, a group effect takes place and the concrete cover delamination is found to be the critical failure mode. Cover delamination can be induced by high bond stress gradient in the laminate-concrete interface, at the extremities of the laminate or due to the formation of an intermediate shear crack in the strengthened element. When this failure occurs, the potential reinforcement that CFRP laminates can provide becomes limited significantly. This loss of efficacy depends on several parameters, such as: distance between laminates [3], concrete strength class, and percentage of conventional longitudinal steel reinforcement. From the design point of view, it is important to take into account this premature and brittle failure mode, and determine guiding parameters for its prediction. This paper presents the results of an experimental program composed by fifteen flexural tests with RC slab strips strengthened with NSM CFRP laminates. The influence of the distance between laminates and, consequently, of the strengthening ratio, on the flexural strengthening efficacy and its dependence on the concrete strength is investigated. The experimental program is described, and the main results are presented and discussed.

2 EXPERIMENTAL PROGRAM

2.1 Specimen and Test Configuration

To assess the influence of the spacing between NSM-CFRP laminates on the flexural strengthening efficacy of RC slabs, the test setup represented in Fig. 1 was used, and the four laminate arrangements, illustrated in Table 1, were adopted. For the purpose of analyzing the dependence of the flexural strengthening efficacy on the concrete strength, three series of RC slabs of distinct concrete strength grades (low, medium and high) were tested.

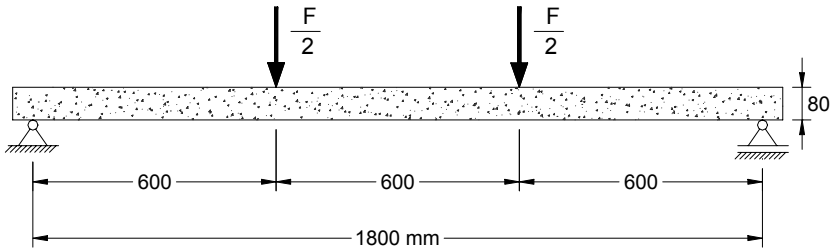

Fig. 1 Test setup configuration (dimensions in mm).

The cross-section dimensions of the tested slab strips are included in Table 1. Here, the equivalent reinforcement ratio is defined as:

$$\rho_{s,eq} = \frac{A_s}{b \cdot d_s} + \frac{E_f}{E_s} \cdot \frac{A_f}{b \cdot d_f} \tag{1}$$

where b is the width of the slab cross section, A_s, E_s, and d_s are the cross-sectional area, the Young's modulus, and the effective depth of the internal steel reinforcement, and A_f, E_f and d_f, are the cross-sectional area, the Young's modulus and the effective depth of the laminates. In this expression $\rho_s = A_s / b \cdot d_s$ is the reinforcement ratio of longitudinal steel bars and $\rho_f = A_f / b \cdot d_f$ is the CFRP strengthening ratio.

Table 1 Details of the specimens cross sections.

Slab specimen	Cross section (dimensions in mm)	No. of laminates	ρ_f (%)	$\rho_{s,eq}$ (%)	$\frac{A_f}{A_s}$ (%)
SO	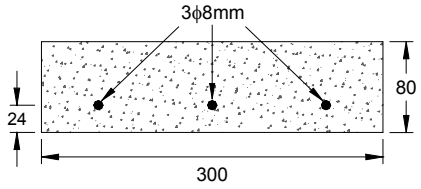	0 (reference)	0	0.90	0
S1	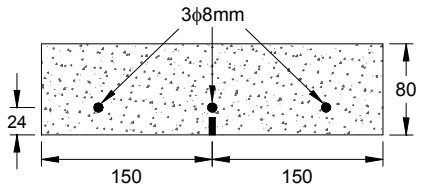	1	0.06	0.95	9.30
S2	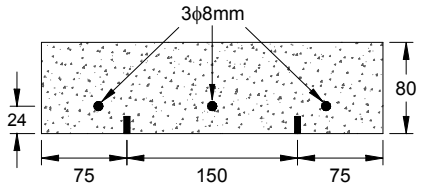	2	0.13	1.00	18.61
S4	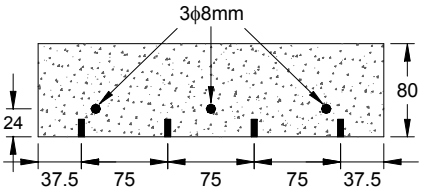	4	0.25	1.10	37.21
S8	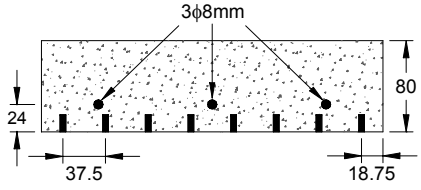	8	0.50	1.30	74.42

2.2 Measuring devices

Fig. 2 depicts the positioning of the sensors for data acquisition. To measure the deflection of the slab strip, five linear voltage differential transducers (LVDT #1 to LVDT #5) were supported in a suspension yoke (see Fig. 2(a)). LVDT #3, placed at the slab strip mid-span, was also used to control the test at 20 μm/s up to the deflection of 49 mm. After this deflection, the actuator internal LVDT was used to control the test at 25 μm/s displacement rate up to the failure of the slab. The total applied

force, F, was measured using a load cell of ±200 kN and accuracy of 0.5%, placed between the loading steel frame and the actuator of 600 kN load capacity.

To measure the strains in the steel reinforcements, two electrical resistance strain gauges (SG1 and SG2) were installed on the internal steel reinforcements, according to the arrangement indicated in Fig. 2(b). Two strain gauges (SG3 and SG4) were bonded on the top concrete surface to determine the maximum concrete compressive strain, Fig. 2(c). Five strain gauges were also installed on one CFRP laminate (SG5 to SG9) for evaluating the strain variation along the laminate, see Fig. 2(d).

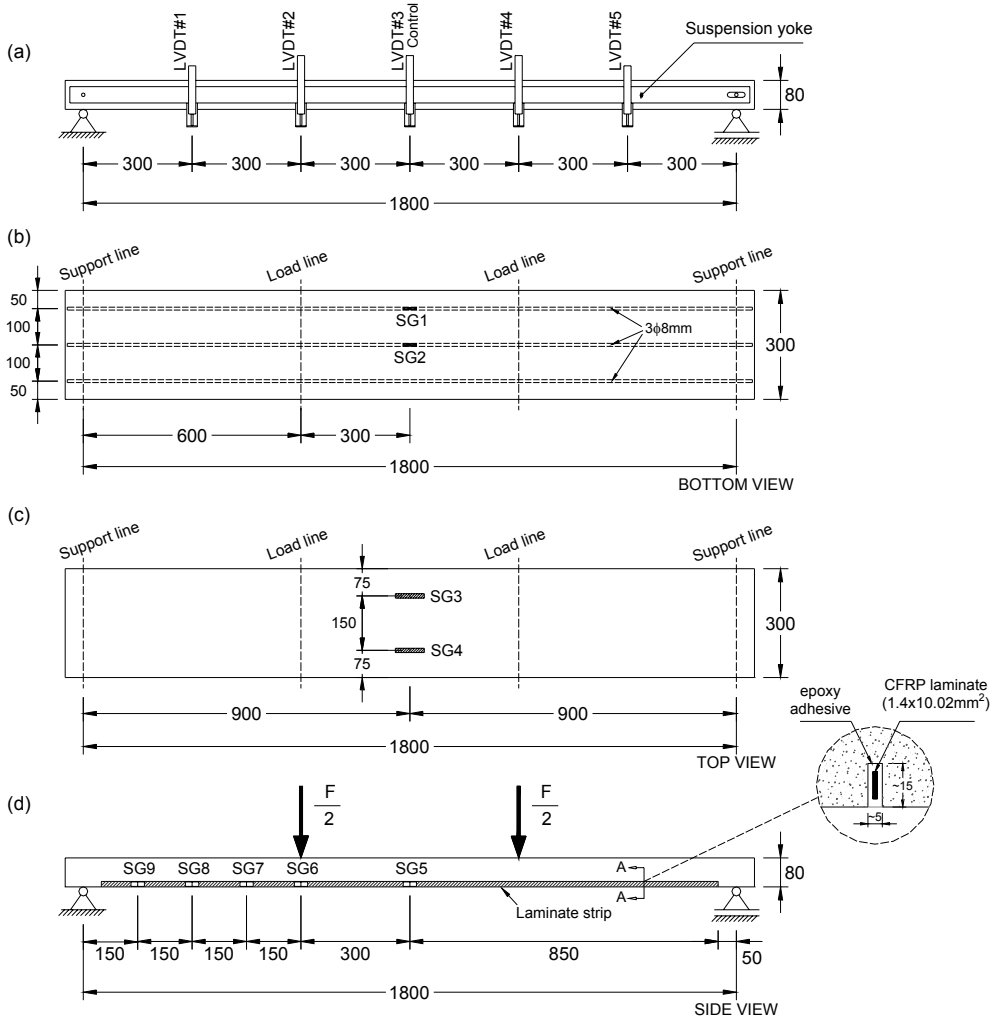

Fig. 2 Arrangement of displacement transducers and strain gauges: (a) displacement transducers; (b) lay-out of the strain gauges at the steel bars - bottom view; (c) strain gauges at the concrete slab top surface - top view; and (d) position of the strain gauges at the CFRP laminate -side view (all dimensions are in mm).

2.3 Materials properties

Table 2 and Table 3 include values obtained from experimental tests carried out to evaluate the main properties of the materials used in the present work.

The main properties of the three classes of ordinary concrete used in this study are shown in Table 2. From four compression tests with cylinder specimens (150 mm x 300 mm), carried out according to EN 12390-3 recommendations [4], at the daytime of the slab test, the average compressive strength (f_{cm}) values indicated in Table 2 were obtained.

To characterize the steel bars, uniaxial tensile tests were conducted according to the standard procedures found in EN 10002-1 [5]. The uniaxial tensile tests on CFRP coupons were carried out according to the ISO 527-5 recommendations [6]. The CFRP laminates were supplied by S&P - Clever Reinforcement Ibérica Company. For the laminate epoxy adhesive, the uniaxial tensile tests were

performed complying with the procedures outlined by ISO 527-2 [7]. The main properties of steel bars, pultruded CFRP laminates and epoxy adhesive are included in Table 3.

Table 2 Characteristics of the ready-mix concretes.

Mix designation	Strength class	Testing age (days)	Apparent gravity (kg/m^3)	f_{cm} (N/mm^2)
C1	C12/16	58	2194	18.85
C2	C35/45	66	2321	41.74
C3	C50/60	59	2380	57.29

Table 3 Summary of the characteristics of the steel reinforcement, laminates and epoxy adhesive.

Steel reinforcement	Pultruded CFRP laminate	Laminate adhesive
ϕ_s = 8 mm E_s = 200.80 GPa σ_{sy} = 438.20 MPa ε_{sy} = 4.20 ‰ σ_{su} = 578.75 MPa e_f = 31.75 % [b]	t_f = 1.40 mm w_f = 10.02 mm E_f = 161.41 GPa ν_f = 0.29 [c] σ_{fu} = 1776.35 MPa ε_{fu} = 11.01 ‰	E_a = 7.47 GPa σ_{au} = 33.03 MPa ε_{au} = 4.83 ‰

[a] Elongation, obtained from measurements over gauge length of $5\phi_s$; [b] Poisson's ratio, determined from axial and transverse extensometers, installed in the tensile coupon [8]

2.4 Results and analysis

2.4.1 Indicators of the NSM efficacy

The load-mid span deflection curves and the relationship between the applied load and the strains recorded in the strain gauges of the tested slabs are presented in Figs. 3, 4 and 5, for the concrete strength class C1, C2 and C3, respectively.

As $F-\delta$ relationships of Figs. 3 to 5 show, that the service load, F_s (the force corresponding to the mid-span deflection of ℓ/250, where ℓ, in mm, is the slab span length), the load at the yielding of the steel reinforcement, F_y, and the maximum load, F_u, all of them increased significantly with the increase of both ρ_f and concrete strength class. Fig. 6 shows that, apart $\Delta F_u / F_u^{Ref}$ of S4 and S8 slabs of C3 concrete strength class, the increase of $\Delta F_s / F_s^{Ref}$ [a], $\Delta F_y / F_y^{Ref}$ and $\Delta F_u / F_u^{Ref}$ had a similar increasing trend with ρ_f for the three considered concrete strength classes. The maximum increment amongst these ratios, which are indicators of the NSM flexural strengthening efficacy, was registered in $\Delta F_u / F_u^{Ref}$ that ranged from 1.8 in the C1 concrete strength class and 3.4 in the C2 and C3 concrete strength classes. In terms of service load, the increment of $\Delta F_s / F_s^{Ref}$ increased almost linearly with ρ_f.

[a] The superscript *Ref* refers to the reference slab.

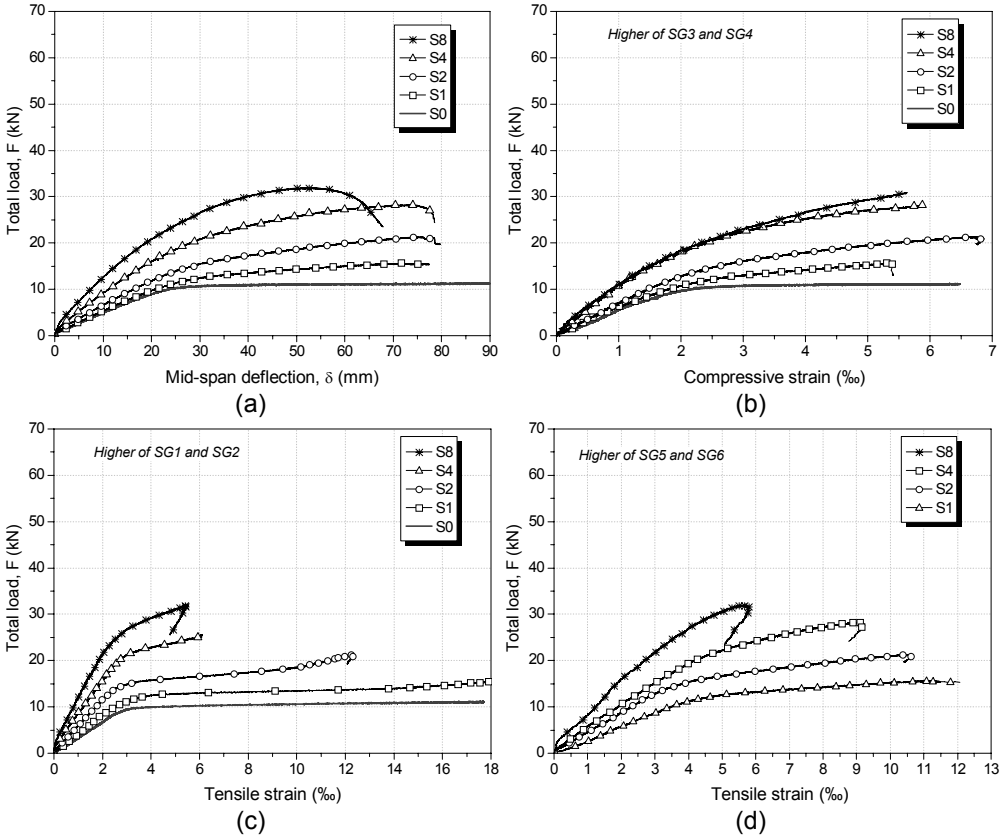

Fig. 3 Results of C1: (a) central deflection; (b) concrete strain; (c) steel strain; and (d) laminate strain.

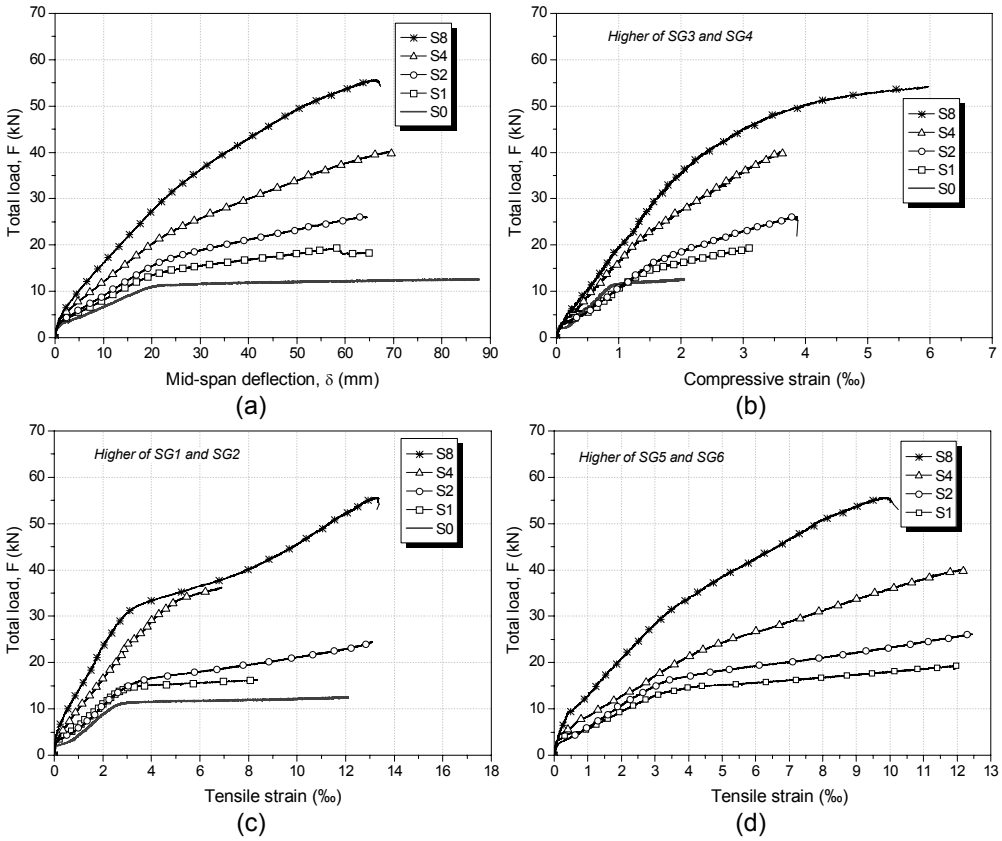

Fig. 4 Results of C2: (a) central deflection; (b) concrete strain; (c) steel strain; and (d) laminate strain.

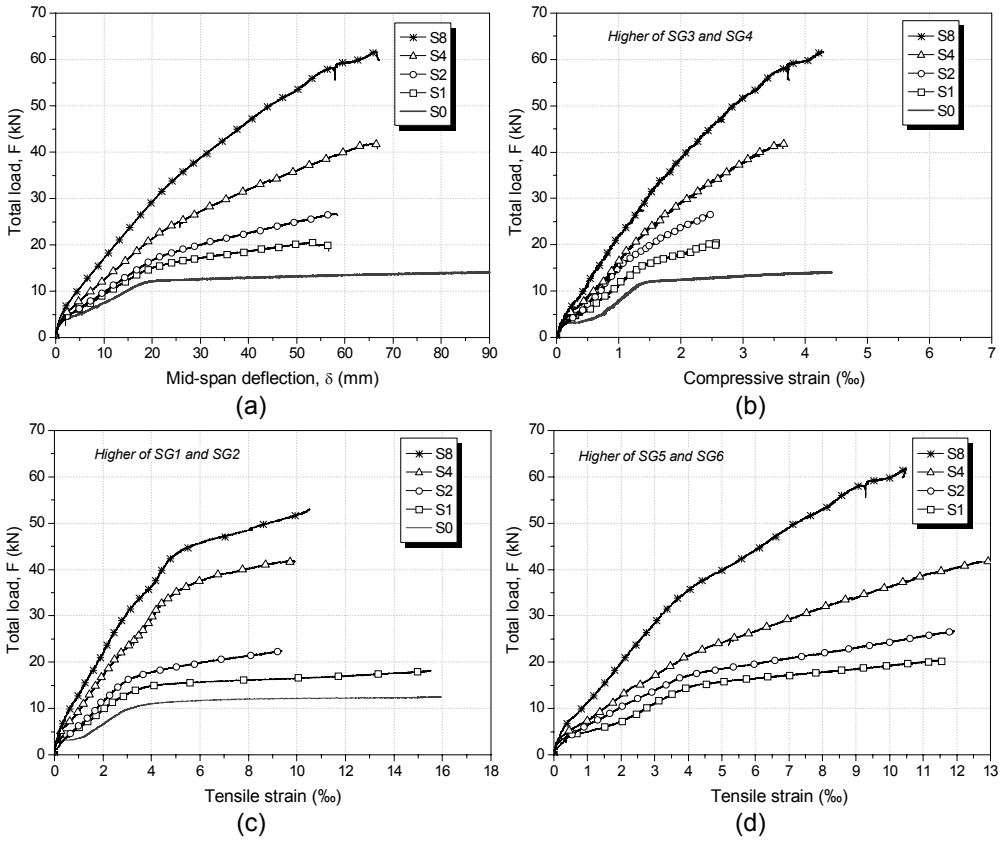

Fig. 5 Results of C3: (a) central deflection; (b) concrete strain; (c) steel strain; and (d) laminate strain.

This means that NSM is a very effective flexural strengthening technique to increase the service load of RC slabs, since the detrimental group effect (premature detachment of a concrete layer that includes the laminates), even for the short distances between laminates such as 37.5 mm, did not occur. In terms of yielding load, the increase of $\Delta F_y / F_y^{Ref}$ with the increment of ρ_f was larger from ρ_f = 0.13% to ρ_f = 0.25% than in the other two intervals. Since F_y is the force when the strains recorded in the SG1 and SG2 strain gauges (see Fig. 2(b)) attained the yield strain registered in the tensile tests with specimens (Table 3), the values of F_y indicated in Fig. 6 can include some error in its evaluation due to the fact that the strains at SG1 and SG2 only represent the strains in the areas where the strain gauges are fixed. Therefore, an almost linear increase trend between F_y and ρ_f is also possible. The increase in terms of maximum load, provided by the increase of ρ_f was similar for the series of slabs of C2 and C3 concrete strength classes. The increase was higher up to ρ_f = 0.25% than for the series with ρ_f larger than this value, which is justified by the distinct failure modes observed in the slabs of C2 and C3 slabs. In fact slab S8 of C2 concrete strength class failed by concrete crushing and slab S8 of C3 concrete strength class failed by the formation of a shear crack when the slab deflection was about 66 mm. These types of failure modes avoided of mobilizing the full tensile capacity of CFRP laminates. The remaining slabs of C2 and C3 series failed by the rupture of the laminates. The increase of $\Delta F_u / F_u^{Ref}$ with ρ_f of the S4 and S8 slabs of C1 concrete strength class was much lesser than the increase registered in the corresponding slabs of C2 and C3 concrete strength classes. Since the strain at concrete strength, which is about 2.2‰ [9], was attained for a relatively low load level (about 19 kN and 19.4 kN for S4 and S8, respectively), the volume of concrete in compression softening behaviour has limited the increase of the load carrying capacity that laminates would provide in S4 and S8 of C1 series if this softening behaviour had not occurred. From

the strain values recorded in the laminates, it can be concluded that apart S2, S4 and S8 of C1 concrete strength class and S8 of C2 concrete strength class that failed due to concrete crushing, and S8 of C3 that failed by the formation of an intermediate shear crack, in the remaining slabs the maximum strain values in the laminates attained its ultimate strain capacity, justifying the type of failure mode occurred in these slabs: rupture of the laminates (see Table 4).

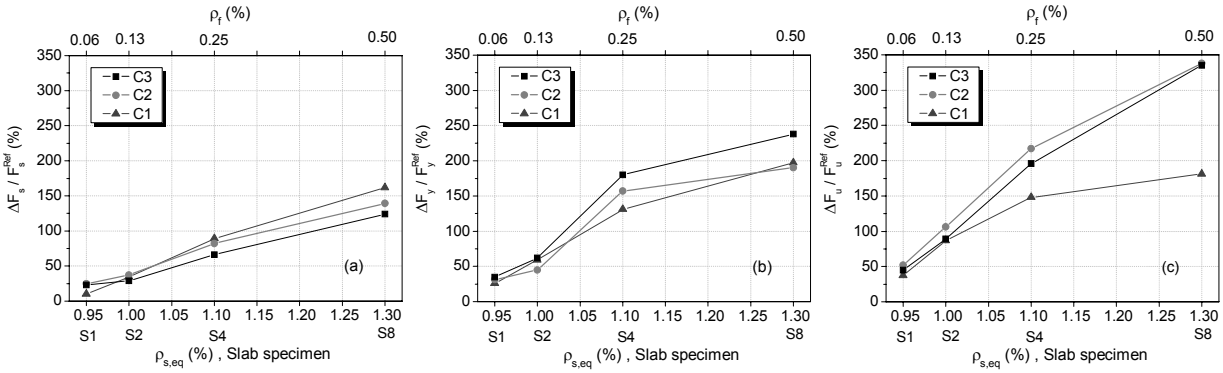

Fig. 6 Load increasing ratio at: (a) service; (b) yielding; and (c) ultimate.

Table 4 Types of failure modes registered.

Slab specimen	Concrete strength class		
	C1	C2	C3
S0	Flexure (yielding of internal reinforcement)	Flexure (yielding of internal reinforcement)	Flexure (yielding of internal reinforcement)
S1	CFRP rupture	CFRP rupture	CFRP rupture
S2	CFRP rupture / concrete crushing at the top	CFRP rupture	CFRP rupture
S4	concrete crushing at the top	CFRP rupture	CFRP rupture
S8	concrete crushing at the top	concrete crushing at the top	Flexo-shear (intermediate shear crack)

Fig. 7(a) compares the maximum values of average bond stress calculated between the SG8-SG7 and SG7-SG6 for all slab specimens of the three considered concrete strength classes. The average bond stress was determined according to the following equation:

$$\tau_{bm}^{RL} = \frac{E_f \cdot A_f \cdot \Delta\varepsilon^{RL}}{2 \cdot w_f \cdot L^{RL}} \text{ (MPa)} \qquad (2)$$

where L^{RL} is the distance between two consecutive strain gauges, SG^L (left) and SG^R (right); $\Delta\varepsilon^{RL}$ is the difference of axial strain between the strain gauge at right and left sections; and A_f, E_f and w_f, are the cross-sectional area, the Young's modulus and the width (Table 3) of the CFRP laminate, respectively.

The comparison of the efficacy ($\varepsilon_{f,max} / \varepsilon_{fu}$) of the four strengthening configurations is depicted in Fig. 7(b). As it appears from the Fig. 7(b) the concrete compressive strength, at the top of the slab, plays the most important role in the efficacy of the strengthening. While in the concrete strength classes C2 and C3 no significant alteration in the strengthening efficacy was observed up to the strengthening ratio of 0.25%, for the concrete of low strength (C1) a sensible reduction in the

strengthening efficacy was verified. This is confirmed by the relationship $\tau_{bm}^{RL} - \rho_{s,eq}$ of C1 curve in Fig. 7(a). The maximum τ_{bm}^{RL} was 4.3 MPa and it occurred in the series of C2 concrete strength class. This bond stress was not high enough to develop a cohesive shear/splitting failure of the concrete surrounding the laminates that occurs when the interference between consecutive laminates is significant and bond stress are too high for the strength of the concrete surrounding the laminates.

2.4.2 Crack patterns

Since the relevant aspects of the crack patterns developed in the tested slabs are common to these slabs, the analysis will be restricted to the crack pattern of C2S1 slab, illustrated in Fig. 8. From this figure it can be seen that a typical crack pattern is composed by primary flexural cracks and secondary debounding cracks. Analysing, for example, for example, analysing the two flexural cracks "A" and "B", that first occurred when the tensile stresses due to bending exceeded the flexural strength of the concrete at the respective sections ("A" and "B"). Upon further increase in the load, these primary cracks, which intercept the laminate, caused the occurrence of slip at the laminate/concrete interfaces[b], and, hence, the formation of small diagonal "branching" cracks around the flexural cracks. These branching cracks are secondary cracks caused by the relative sliding between the laminates and the adjacent concrete [10,11]. The formation of secondary cracks propagated, in each flexural crack, in both directions such as from A_0 to B' and from A_0 to A' (see Fig. 8). In-between the primary flexural cracks "A" and "B", the secondary cracks propagate in both direction, from A_0 to B' and from B_0 to A'. This "branching" behaviour is consistent with the characteristic herringbone formation of cracks associated with shear cracking in concrete members [10,12]. In the present case, the secondary cracks have the inclination of the principal tensile stress that exceeded the local concrete tensile strength, caused by the bond stresses transferred between laminate and surrounding concrete during the sliding procedure of the laminate. Hence, there is reversal in slip and bond stress between two consecutives primary flexural cracks and a point of zero slip occurs between them. In the tests it was found that most of the flexural cracks formed up to the load levels corresponding to the yielding of the internal steel reinforcement, principally in-between the applied line loads ("pure" moment region). The major part of the branching cracks, that get a herringbone crack configuration, were formed after these load levels, due to the relative sliding between the laminates and the adjacent concrete.

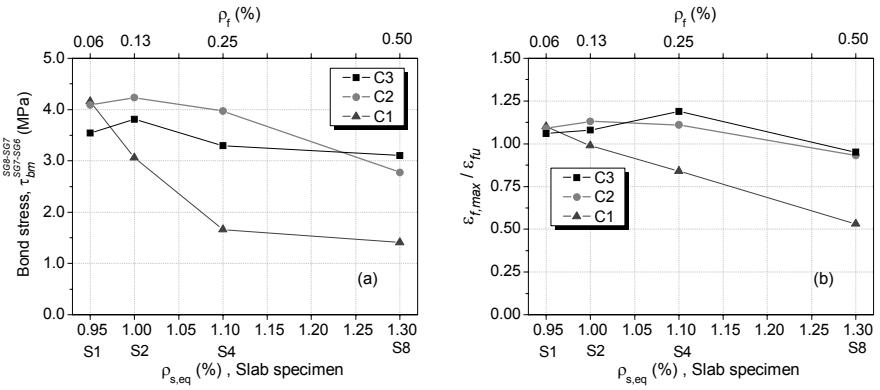

Fig. 7 (a) comparison of the maximum average bond stress between the SG8-SG7 and SG7-SG6; and (b) CFRP laminate efficiency factor.

From the tests, for a loading stage close to the maximum applied load it was verified that increasing the percentage of laminates, the cracking phenomenon, at the soffit of the slab, is degenerated in a multicracking pattern with much more closely-spaced cracks and no visible formation of herringbone crack configuration (see Fig. 8). This behaviour was more evident in the slabs with high percentage of laminates (C1S8, C2S8 and C3S8 slabs).

[b] In this context, the slip between the laminate and the epoxy adhesive is not considered, and the assembled CFRP laminate and the two adhesive walls, inside the slit, are referred to as laminate.

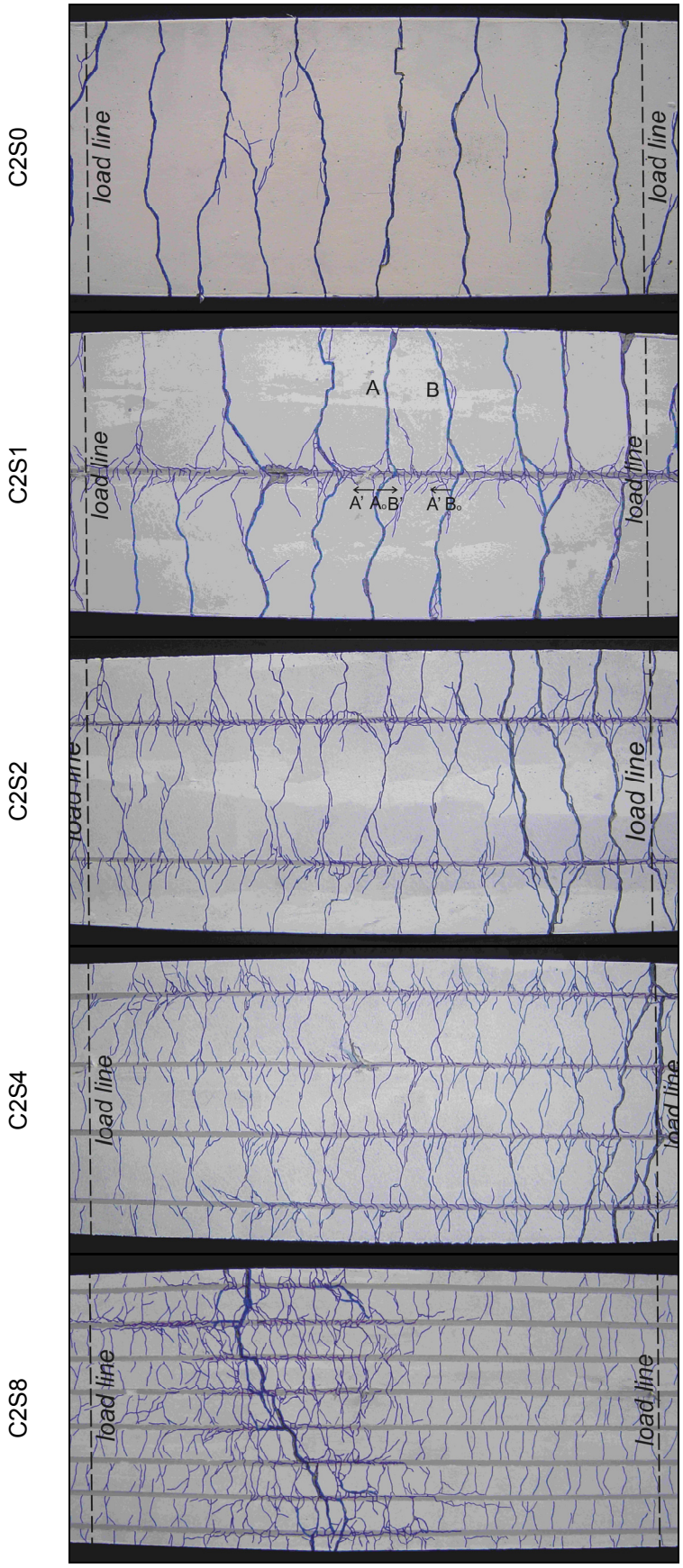

Fig. 8 Crack pattern recorded after testing in the constant moment zone (600 mm) for class C2.

When the spacing between adjacent laminates decreases the direction of principal tensile stress in the concrete surrounding the laminate is almost coinciding with the direction of the laminates. In the limit, the strengthened concrete cover can be regarded as a membrane submitted to almost uniform tensile strain field.

In this case, an infinite number of cracks were formed, orthogonally to the laminates. In RC members strengthened with NSM laminates, the cracking behaviour is affected, among others, by: (1) the percentage of laminate, which controls the spacing between first major cracks; and (b) the deformations on the CFRP strengthening, which tend to control the crack width of these major cracks (and tempering the formation of herringbone cracks) by limiting the slip between the adjacent concrete and the laminate.

3 CONCLUSIONS

An experimental program was conducted in order to: (a) investigate the influence of the distance between laminates (and, consequently, of the strengthening ratio, ρ_f) on the flexural strengthening efficacy, and (b) evaluate its dependence on the concrete strength. For this purpose a total of fifteen slabs were tested. The following conclusions can be drawn from this experimental study.

For RC slabs of low concrete strength class, such is the case of C12/16, the maximum increment in terms of the slab load carrying capacity is limited by the concrete crushing. However, even for this type of concrete strength class, slabs having longitudinal steel reinforcing ratios do not exceeding 0.90% (the one studied in the present work) can have an increase in terms of load carrying capacity larger than 170% when the unstrengthened slab is taken for basis of comparison. For the slabs reinforced with low concrete strength class, economical reasons advise do not exceeding a CFRP strengthening ratio of 0.13%, which limits the increment of the slab load carrying capacity to 87%, which was still very appreciable. If higher increments are necessary, it is advisable to apply a thin concrete overlay of compressive strength higher than the one of the concrete substrate, as was proven in a previous work. From the results it was observed that, even for reinforced slabs of relatively low concrete strength class, the increment in terms of load for deflection serviceability limit state analysis, provided by ρ_f = 0.13%, 0.25%, and 0.50%, was very significant: 34%, 89%, 162%. The increment for the load corresponding to the onset of the yielding of the longitudinal steel reinforcement was also very appreciable: 26%, 59%, 131%, 197% for ρ_f = 0.06%, 0.13%, 0.25%, and 0.50%.

For the reinforced slabs of C35/45 and C50/60 concrete strength classes, in general, the maximum increment provided by the used ρ_f was limited by the tensile capacity of the laminates, since, apart two cases, the remaining slabs failed by the rupture of the laminates. The maximum increment of ultimate load (338%) provided by a strengthening ratio of 0.50% on slabs of C35/45 concrete strength class was conditioned by the concrete crushing. In the case of the reinforced slab of C50/60 concrete strength class, strengthened with the maximum ρ_f (0.50%), the maximum increment of ultimate load (335%) was conditioned by the shear resistance of the RC slab. The increment in terms of service load provided by ρ_f = 0.06%, 0.13%, 0.25%, and 0.50% in reinforced slabs of C35/45 and C50/60 concrete strength classes was about 25%, 37%, 82%, 139% and about 23%, 29%, 66%, 124%, respectively. In terms of load at the yielding of the reinforcement, strengthening ratios of ρ_f = 0.06%, 0.13%, 0.25%, and 0.50% in slabs of these two types of concrete strength classes was provided an increment of about 31%, 45%, 157% and 190% and about 35%, 62%, 180%, 238%, respectively.

The type of failure mode reported in some experimental and numerical research works dealing with the NSM for RC beams, and consisting on the detachment of a concrete layer that includes the laminates, never occurred in the present experimental program, even for a spacing between laminates of 37.5 mm, which is already a too small distance between laminates, when considering economical reasons. This indicates that NSM is especially appropriate to increase the flexural resistance of RC slabs. However, the influence of the reinforcement ratio of existent longitudinal steel bars and the relative position between laminates and steel bars should be also investigated to define confident and well sustained design guidelines.

Finally, the post-inspection of the crack patterns of the tested slabs showed that the distance between cracks decreased with the increase of ρ_f, independently of the concrete strength class. This

leads to an important benefit in terms of structural durability, since for a certain load level the crack width is so low as larger is ρ_f, resulting higher resistances to the propagation of the phenomena conducting to the corrosion of the internal steel bars

ACKNOWLEDGEMENTS

The authors acknowledge the financial support of the Portuguese Science and Technology Foundation (FCT), PhD grant number SFRH / BD / 11232 / 2002. Thanks also for the companies "Companhia Geral de Cal e Cimento S.A. (SECIL)", Civitest Lda, "Degussa Construction Chemicals Portugal S.A.", S&P® Clever Reinforcement Iberica Lda, which generously have supplied the ready mix concretes; the installations to work, the CFRP adhesive product; and the CFRP laminate, respectively.

REFERENCES

[1] Barros, J.A.O., Dias, S.J.E., and Lima, J.L.T., "Efficacy of CFRP-based Techniques for the Flexural and Shear Strengthening of Concrete Beams", *Cement and Concrete Composites* (in press), 2006.

[2] Barros, J.A.O., Dias, S.J.E., "Near Surface Mounted CFRP Laminates for Shear Strengthening of Concrete Beams", *Cement and Concrete Composites*, 28, 3, 2006, pp. 276-292.

[3] Kang, J.-Y., Park, Y.-H., Park, J.-S., You, Y.-J., and Jung, W.-T., "Analytical Evaluation of RC Beams Strengthened with Near Surface Mounted CFRP Laminates", *7th International Symposium on FRP Reinforcement for Concrete Structures*, FRPRCS-7, Kansas City, MO, USA, 2005, pp. 779-794.

[4] NP-EN 12390-3, "Testing Hardened Concrete - Part 3: Compressive Strength of Test Specimens", European Standard, CEN, Brussels, Belgium, 2003.

[5] NP-EN 10 002-1, "Metallic Materials - Tensile Testing. Part 1: Method of Test (at ambient temperature)", European Standard, CEN, Brussels, Belgium, 1990, 35 pp.

[6] ISO 527-5, "Plastics - Determination of Tensile Properties - Part 5: Test Conditions for Unidirectional Fibre-reinforced Plastic Composites", *International Organization for Standardization (ISO)*, Geneva, Switzerland, 1997, 9 pp.

[7] ISO 527-2, "Plastics - Determination of Tensile Properties - Part 2: Test Conditions for Moulding and Extrusion Plastics", *International Organization for Standardization (ISO)*, Geneva, Switzerland, 1993.

[8] ASTM D3039/D3039M, "Standard Test Method for Tensile Properties of Polymer Matrix Composite Materials", *ASTM International*, 2000, 13 pp.

[9] CEB-FIB, *Model code 1990*, Thomas Telford, London, 1990.

[10] Liu, I.S.T., Oehlers, D.J. and Seracino, R., "Tests on the Ductility of Reinforced Concrete Beams Retrofitted with FRP and Steel Near-surface Mounted Plates", *Journal of Composites for Construction*, 10, 2, 2006, pp. 106-114.

[11] CIDAR, *Design Guidelines for RC Structures Retrofitted with FRP and Metal Plates: Beams and Sabs*, 2006,109 pp.

[12] Piotter, J.M., "Longitudinal slab splitting in composite girders", *MSc Thesis*, Blacksburg, VA, April 2001.